



Cite this: DOI: 10.1039/c7cy00512a

Brønsted acidic ionic liquid-catalyzed dehydrative formation of isosorbide from sorbitol: introduction of a continuous process†

Jie Deng,^{‡a} Bao-Hua Xu,^{§b} Yao-Feng Wang,^b Xian-En Mo,^{§b} Rui Zhang,^{*a}
You Li^{§b} and Suo-Jiang Zhang^{§b}

A highly efficient synthesis of isosorbide from sorbitol was developed using Brønsted acidic ionic liquids (BILs) as the catalyst for the first time. The structure–performance relationship was discussed extensively and a proper value of the Gutmann acceptor number (AN) rather than the inherent of acidity was found to be essential for an optimized yield of isosorbide. In addition, the excellent behavior of preferred BIL-4 in the consecutive recycling tests renders the construction of a continuous process probable. Systematic optimization demonstrated that a yield of 82% of isosorbide with a purity of 99.3% could be reached at balance.

Received 16th March 2017,
Accepted 5th April 2017

DOI: 10.1039/c7cy00512a

rsc.li/catalysis

Introduction

Isosorbide is one of the most high-value chemicals arising from biomass transformation and has wide applications in the synthesis of several pharmaceutical molecules,¹ fine chemicals² and various polymers.³ Recent reports by Mitsubishi demonstrated the promise of isosorbide to replace bisphenol A in the synthesis of polycarbonate with excellent optical properties.⁴ However, the challenge in promoting such technologies using isosorbide as the synthon is the high cost of isosorbide (more than 10 times that of bisphenol A) resulting from low efficiency and high-energy consumption of production.⁵ The most notable reaction is the dehydration of sorbitol, which is the final step of industrial process for isosorbide from starch. It is an acid-catalyzed pathway, involving the preferential protonation of the primary hydroxyl group (at C1 position), followed by cyclization with the carbon atom at the C4 position. A second protonation of the last primary hydroxyl group at the C6 position and cyclization with the carbon atom at the C3 position leads to the formation of the second ring of isosorbide.⁶ In the in-

dustry, a sulphuric acid catalyzed batch reaction is popular. However, it has serious drawbacks of environmental pollution arising from base–acid neutralization post-treatment, significant handling risk, corrosive nature of the catalyst and stability issues of the products.⁷ To address these issues, considerable efforts have been made for the development of practical and efficient strategies.⁸ The most attractive solution is to design a proper solid acid as the catalyst and thereby construct a continuous manufacturing process attributed to convenient catalyst separation from reaction system.⁹ However, the results of such systems still lack practical value because of the requirement of a high reaction temperature,^{10–12} long reaction time,¹³ abundant catalyst loading¹¹ and limited yield of isosorbide as well.^{14,15} In other words, the dehydration efficiency is reduced remarkably in the case of a heterogeneous catalytic pathway.

Brønsted acidic ionic liquids (BILs), on introducing Brønsted substituents into the cation/anion of the ionic liquids (ILs), show flexible acidity, which can be regulated accordingly by functionalizing the organic backbone.¹⁶ BILs have attracted special attention for use as efficient catalysts for the synthesis of valuable chemicals in reactions, such as alkylation, esterification, condensation and rearrangement reactions.¹⁷ For example, the acid-catalyzed dehydration of fructose to 5-hydroxymethylfurfural was explored extensively using BILs as a catalyst, which allowed the reaction to proceed more rapidly with high yields under mild conditions (around 100 °C, ordinary pressure).¹⁸ Importantly, BILs were used to replace conventional mineral acids as the liquid catalyst due to their advantages of non-volatility and non-corrosivity, which enabled catalyst recycling.¹⁹ We, therefore, envisioned that a continuous process leading to isosorbide from sorbitol can be constructed using –SO₃H-based

^a State Key Laboratory of Chemical Engineering, East China University of Science and Technology, Shanghai 200237, China

^b Beijing Key Laboratory of Ionic Liquids Clean Process, Key Laboratory of Green Process and Engineering, State Key Laboratory of Multiphase Complex Systems, Institute of Process Engineering, Chinese Academy of Sciences, Beijing 100190, PR China. E-mail: sjzhang@ipe.ac.cn, r.zhang@ecust.edu.cn

† Electronic supplementary information (ESI) available. CCDC 1523385. For ESI and crystallographic data in CIF or other electronic format see DOI: 10.1039/c7cy00512a

‡ On leave to Institute of Process Engineering.

§ Dynamics simulation and system integration.

BILs as the catalyst. However, the challenge remains in searching a proper structure of BIL to retain a relatively fast rate in the formation of adducts with 1,4-sorbitan, as illustrated by Fukuoka and co-workers.²⁰ Further understanding of the structure–performance relationship, particularly in terms of the second dehydration, deserves further investigation.

Experimental

All reagents were used as received from Acros or Alfa Aesar. Solvents (AR grade) were commercially available unless otherwise stated.

Synthesis

Preparation of BILs. The preparation of BIL-1–8 was achieved by two general steps: formation of the corresponding zwitterionic precursor and subsequent protonation by various mineral acids, whereas BIL-9 was provided by double replacement between its chloride counterpart and $\text{CF}_3\text{SO}_3\text{H}$.²¹ To obtain BILs of extreme purity, it is essential to wash the raw products repeatedly with dry diethylether, followed by dehydration under high vacuum (10 Pa) at 80 °C for 24 h. All BILs, except BIL-1, 2 and 9, were treated with active carbon to remove the colored impurities. In addition, care was taken for the preparation of BIL-2 and BIL-9, which are potentially sensitive to moisture and temperature. The quality of BILs under study was characterized by a combination of NMR spectroscopy, Karl Fisher titration, acid–base titration, ESI detection, and TGA analysis. *Caution: The moisture concentration ($\chi_{\text{H}_2\text{O}}$: $n_{\text{water}}/n_{\text{IL}}$) of these neat BILs is controlled to be less than 2×10^{-3} determined by Karl Fischer titration.* For the detail synthetic method and characterization data, see the ESI.† All of the BILs were stored in glass vials in an argon-filled glovebox (<0.1 ppm H_2O) at 25 °C.

Catalytic reaction. The reactions were carried out in a three-necked flask (50 mL) equipped with a vacuum distillation apparatus and a magnetic stirrer. Sorbitol (36.4 g, 0.2 mol) was stirred and heated to 130 °C until it completely melted and became transparent within 30 min. The respective neat BIL (1.2 mmol, 0.6 mol%) was added to the flask with continuous stirring and the pressure was kept at 3 kPa. This time was assigned as $t = 0$ h. After a reaction for 4 h, the pressure was recharged to 1 atm. The products-distribution of the resulting solution was analyzed by HPLC.

Dynamic experiments. Sorbitol (36.4 g, 0.2 mol) was stirred and heated to a temperature at which it completely melted. The respective neat BIL-4 (0.42 g, 1.2 mmol, 0.6 mol%) was added to the flask under continuous stirring and kept at a pressure of 3 kPa. This time was assigned as $t = 0$ h. Liquid samples of a few milligrams were withdrawn and analyzed by HPLC.

Recycling experiments. In the typical recycling experiment, a mixture of sorbitol (91.0 g, 0.5 mol) and neat BIL-4 (1.06 g, 3.0 mmol, 0.6 mol%) was added in a three-necked flask (100 mL, W^0) equipped with a vacuum distillation apparatus and a magnetic stirrer. The mixture was stirred vigorously at 130

°C for 30 min, followed by reaction for 4 h, under 3 kPa. The pressure was then recharged to 1 atm, the total mass of the flask was recorded as W^n and liquid sample of a few milligrams (w^n) was withdrawn and analyzed by HPLC. The reaction solution was then divided into two components upon treatment at 170 °C under 9–15 Pa, with only a part of isosorbide (W_{iso}^n) being distilled. The mass of residue was recorded as $W^{n'}$; a liquid sample of a few milligrams ($w^{n'}$) was withdrawn and analyzed by HPLC. Thereafter, fresh sorbitol ($W_{\text{sor}}^{(n+1)}$) was added to the flask for the next run.

Procedures for HPLC analysis: The sample obtained from the reaction, such as w^n and $w^{n'}$, was dissolved in water (4 mL). The peak areas of sorbitol (S_{sor}^n) and isosorbide (S_{iso}^n) were determined by HPLC analysis. Thereafter, the molar concentration of each (C_{iso} and C_{sor} (mM)) was obtained according to eqn (1) and (2) arising from a linearity fitting standard curve.

$$C_{\text{iso}}^{n/n'} = 5.58 \times 10^{-4} S_{\text{iso}}^{n/n'} + 1.8 \quad (\text{R-Square: } 0.99945) \quad (1)$$

$$C_{\text{sor}}^{n/n'} = 3.98 \times 10^{-4} S_{\text{sor}}^{n/n'} + 0.92 \quad (\text{R-Square: } 0.99962) \quad (2)$$

For run 1:

$$C_{\text{sor}}^1 = 1 - [4(W^1 - W^0)C_{\text{sor}}^1/w^1]/0.5 = 1 - 8(W^1 - W^0)C_{\text{sor}}^1/w^1$$

$$Y_{\text{iso}}^1 = [4(W^1 - W^0)C_{\text{iso}}^1/w^1]/0.5 = 8(W^1 - W^0)C_{\text{iso}}^1/w^1$$

For run n :

$$W_{\text{sor}}^n = (W_{\text{iso}}^{(n-1)}/M_{\text{iso}}) \times M_{\text{sor}} (M_{\text{iso}} = 146; M_{\text{sor}} = 182)$$

$$C_{\text{sor}}^n = 1 - [4(W^n - W^0)C_{\text{sor}}^n/w^n]/[W_{\text{iso}}^{(n-1)}/M_{\text{iso}} + 4(W^{(n-1)'}/W^0)C_{\text{sor}}^{(n-1)'}/w^{(n-1)'}]$$

$$Y_{\text{iso}}^n = 4[(W^n - W^0)C_{\text{iso}}^n/w^n - (W^{(n-1)'}/W^0)C_{\text{iso}}^{(n-1)'}/w^{(n-1)'}]/[W_{\text{iso}}^{(n-1)}/M_{\text{iso}} + 4(W^{(n-1)'}/W^0)C_{\text{sor}}^{(n-1)'}/w^{(n-1)'}]$$

Analysis

HPLC chromatography. HPLC analysis was performed using a Phenomenex Rezex RCM-monosaccharide column (8%; Ca^{2+} , 300×7.80 mm) at 80 °C, with degassed demi water as the eluent using a differential refractive index as the detector.

NMR spectroscopy. For NMR of neat ionic liquids, each dry ionic liquid was loaded into NMR tubes with d_6 -dimethylphosphine as an external lock. The ^1H NMR spectra were recorded using a Bruker Avance III 600 MHz spectrometer.

Acceptor number determination. The method for obtaining the AN value of each BIL is reported

elsewhere.^{16c,22} For each BIL, three samples with different triethylphosphine oxide (TEPO) concentrations (3–10 mol%) were prepared in a glovebox. The solutions were loaded into NMR tubes (after ensuring TEPO dissolution) containing sealed capillaries with *d*₆-dimethylsulfoxide as an external lock. The ³¹P{¹H} NMR spectra were recorded at 80 °C, using a Bruker AvanceIII 600 MHz spectrometer.

Three solutions of TEPO in extremely dry hexane were measured at 27 °C. For each TEPO ionic liquid system, the ³¹P{¹H} NMR chemical shift for the infinite dilution of TEPO, δ_{inf} , was determined by extrapolation from the ³¹P{¹H} NMR chemical shifts measured at different TEPO concentrations. The chemical shift of TEPO in hexane, extrapolated to infinite dilution, $\delta_{\text{inf hex}}$, was used as a reference ($\delta_{\text{inf hex}} = 0$ ppm).

The AN values for all samples were calculated using the following formula: $\text{AN} = 2.348 \times \delta_{\text{inf}}$.

Results and discussion

Synthesis and catalytic performance

BIL synthesis. To explore structure–performance relationship, readily tunable imidazolium was selected as the backbone of BILs to be screened. As depicted in Fig. 1, considerations in terms of the structural design included the anion types, the substituents on the C2–H position, the length of hydrophobic chain, and the functionalization/length of the bridge chain.

A series of BILs were synthesized (Fig. 2). The preparation of BIL-1–8 was achieved by two general steps: formation of the corresponding zwitterionic precursor and subsequent protonation by various mineral acids. In contrast, BIL-9 was provided by double replacement between its chloride counterpart and CF₃SO₃H.²¹ The preparation of BIL-1–8 was achieved by two general steps: formation of the corresponding zwitterionic precursor and subsequent protonation by various mineral acids. However, BIL-9 was provided by double replacement between its chloride counterpart and CF₃SO₃H.²¹ Monitored by acid–base titration, full protonation or replacement was obtained with all mineral acids except the relatively weak HCl. Evidently, the corresponding BIL-1 of fresh preparation only consumes 40 mol% of NaOH at room temperature. On the other hand, the titration value of approximately 2 for BIL-3 is rationalized by the reactivity of its two subunits, –SO₃H and HSO₄[–], towards NaOH. An extra

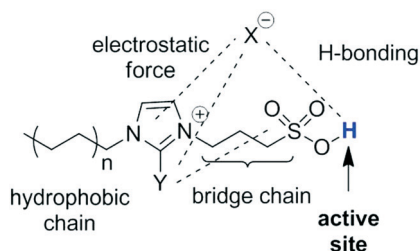


Fig. 1 Schematic of the structural consideration for BIL.

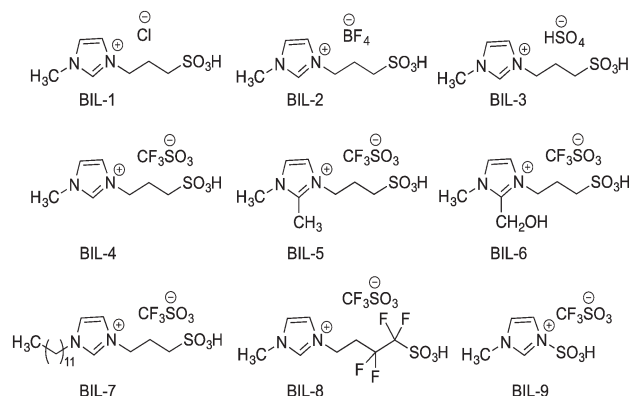


Fig. 2 BILs prepared and screened as the catalyst.

equivalent of NaOH consumption was also detected for BIL-2 and BIL-9. Cross experiments attributed it to the respective hydrolysis of BF₄[–] in BIL-2 (ref. 23) and weak N–S bond in BIL-9 (ref. 21) under strongly basic conditions (Table S1†). In the experiments, such instability of BIL-2 and BIL-9 against moisture was also detected during their respective preparation or storage. Therefore, additional care was taken when either BIL-2 or BIL-9 was introduced as a catalyst in the presence of H₂O, particularly at high temperatures. Thermogravimetric analysis (TGA) with scanning rate of 10 °C min^{–1} was also conducted for BIL-2–9, indicating that these BILs are thermally stable (*T*_d > 300 °C, Fig. S1†) enough for the catalytic conversion of sorbitol to isosorbide.

Catalytic reactions. The catalytic performance of these characterized BILs was subsequently evaluated (Table 1). The moisture content ($\chi_{\text{H}_2\text{O}} = n_{\text{water}}/n_{\text{H}}$) in each BIL under study was less than 2×10^{-3} , as determined by a Karl Fischer titration. All reactions were conducted in the presence of BIL (0.6 mol%) under vacuum (3 kPa) at 130 °C for 4 h, by generating a mixture of 1,4-sorbitan and isosorbide as the major product, together with traces of others upon dehydration, such as 1,5-sorbitan and 3,6-sorbitan. In addition, the performance of two mineral acids, H₂SO₄ and CF₃SO₃H, was also studied for comparison.

As listed in Table 1, the performance of these screened BILs is nearly the same in the first dehydration; however, it varies significantly in the second. The efficiency of dehydration was increased upon adjusting the anionic structure of BILs, displaying an order of BF₄[–] < HSO₄[–] < CF₃SO₃[–]. The activity of BIL-3 (entry 2) is comparable to that of the commercial catalyst (H₂SO₄, entry 9) under identical conditions. In contrast, the second dehydration proceeded efficiently in the presence of BIL-3 (entry 3) compared with that of its anionic counter-acid (CF₃SO₃H, entry 10). The reactivity was increased when the strength of the H-donor at the C2-position was weakened, as presented by BIL-4/6 versus BIL-5 (entries 3–5). Unfortunately, the yield of isosorbide was not improved further by rendering the amphipathic BIL either more hydrophobic (BIL-7, entry 6) or more strongly acidic (BIL-8, entry 7). Finally, BIL-9, in which the imidazole ring was substituted directly with sulfonic acid group, behaved sluggishly, partially arising from its instability.

Table 1 BILs-catalyzed dehydrative formation of isosorbide from sorbitol^{a,c}

Entry	Cat.	Conv. ^b (%)	Y _{Sorbitan} ^b (%)	Y _{Isosorbide} ^b (%)
1	BIL-2	91.5 (±1.0)	76.5 (±2.5)	11.8 (±2.0)
2	BIL-3	98.0 (±1.0)	53.3 (±2.3)	40.5 (±2.0)
3	BIL-4	98.3 (±0.8)	10.3 (±2.3)	75.5 (±1.0)
4	BIL-5	99.8 (±0.8)	4.3 (±1.5)	84.5 (±1.0)
5	BIL-6	98.0 (±0.5)	37.0 (±0.5)	55.0 (±1.0)
6	BIL-7	99.8 (±0.8)	8.3 (±0.8)	77.3 (±1.3)
7	BIL-8	98.8 (±0.8)	38.3 (±1.9)	62.8 (±1.9)
8	BIL-9	98.8 (±0.4)	66.5 (±1.0)	21.8 (±1.8)
9	H ₂ SO ₄	97.5 (±0.5)	56.8 (±0.8)	34.5 (±1.0)
10	CF ₃ SO ₃ H	98.0 (±0.5)	77.8 (±0.9)	16.8 (±0.8)

^a Reaction conditions: sorbitol 0.2 mol, catalyst 0.6 mol%, 130 °C, 3 kPa, 4 h. ^b Determined by HPLC with a Phenomenex Rezex RCM-monosaccharide column (8%; Ca²⁺, 300 × 7.80 mm) at 80 °C, degassed demi water as eluent. ^c The formation of punds could not be completely ruled out.

Characterization and structure–performance relationship

To address the above issue of remarkably different performance of BILs in the second dehydration, structures of neat BILs and their ability to protonate nucleophiles were examined *via* a combination of ¹H NMR and Gutmann acceptor number (AN).

Interaction between BIL and nucleophilic H₂O. The difficulty in removing traces of H₂O from BILs is because of their extensive interactions arising from H-bonding.²⁴ Consequently, significant care should be taken when preparing these BILs and applying in dehydrated reactions as well. The $\chi_{\text{H}_2\text{O}}$ –acidity plot and acceptable $\chi_{\text{H}_2\text{O}}$ for a neat BIL should be defined before respective structural analysis. Therefore, ¹H NMR detection of a mixture of BIL-4 and H₂O in a variant ratio was conducted using DMSO-*d*₆ as an external lock. As indicated in Fig. 3, the value of both chemical shift and labile proton integration depends on the value of $\chi_{\text{H}_2\text{O}}$. There is an up field shift of the labile proton of –SO₃H accompanied by increasing $\chi_{\text{H}_2\text{O}}$, and a significant reduction of δ (ppm) is observed within a range of $0 < \chi_{\text{H}_2\text{O}} < 15$, followed by a steady δ

value around 4 ppm. This was attributed to proton exchange between –SO₃H and H₂O, which approaches equilibrium with a certain amount of H₂O. In addition, we were able to detect a linear dependence of the integration of labile proton on $\chi_{\text{H}_2\text{O}}$. It is likely that a multi-nuclear complex of [SO₃–H(H₂O)⋯anion] for BIL was generated in the presence of H₂O. Even so, the effect of H₂O on the BIL property could be considered negligible when $\chi_{\text{H}_2\text{O}}$ is controlled to be less than 2×10^{-3} , which was used in the catalytic reaction and subsequent structural analysis, unless otherwise stated.

¹H NMR spectroscopy of neat BILs. The labile proton in BILs is potentially involved in a H-bond with two H-acceptors: the anion (X) and alkyl sulfonate anion (–RSO₃[–]), each instantaneously H-bonds with imidazolium cation *via* C2–H. NMR studies were carried out for neat BIL-2–9 but BIL-7, which was solid at the experimental temperature (80 °C). The measurement was carried out using DMSO-*d*₆ as an external lock to evaluate the inherent H-bond strength raised by the labile protons. The most downfield signal (δ : ppm) of BIL-2 (10.43), BIL-4 (11.81), and BIL-8 (14.51) corresponds to the proton of the –SO₃H group, respectively (Fig. 4). This is indicated either replacing BF₄[–] by CF₃SO₃[–] or functionalizing the bridge chain with an electron-withdrawing fluorine group renders the labile proton more deshielded. The decreased chemical shift demonstrates that its assigned proton is partaking in H-bond with a stronger H-acceptor. The chemical shift of BIL-5, bearing C2–CH₃ *versus* C2–H, is further downfield shifted (δ : 11.93 ppm) compared to that of BIL-4. It is likely that the weak interaction between the anion and imidazolium-ring resulted in stronger H-bonding between the anion and the active proton in –SO₃H.

The most downfield-shifted signal (δ : ppm) for BIL-3 (12.20) and BIL-6 (7.23), each integrated to two protons, was located on their respective multi-nuclear cluster (Fig. 5). In BIL-3, protons represented in [(HSO₄)(HSO₃(CH₂)_{*n*}–)] are deshielded relative to –SO₃H proton either in BIL-2 or BIL-4.

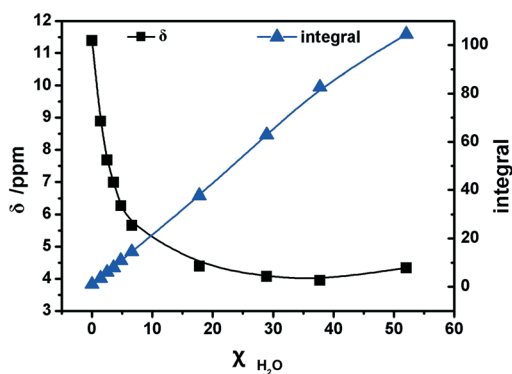


Fig. 3 Variation of the ¹H NMR signal of labile proton in BIL-4 with $\chi_{\text{H}_2\text{O}}$ (detected by ¹H NMR (600 MHz, external DMSO-*d*₆ lock, 80 °C)).

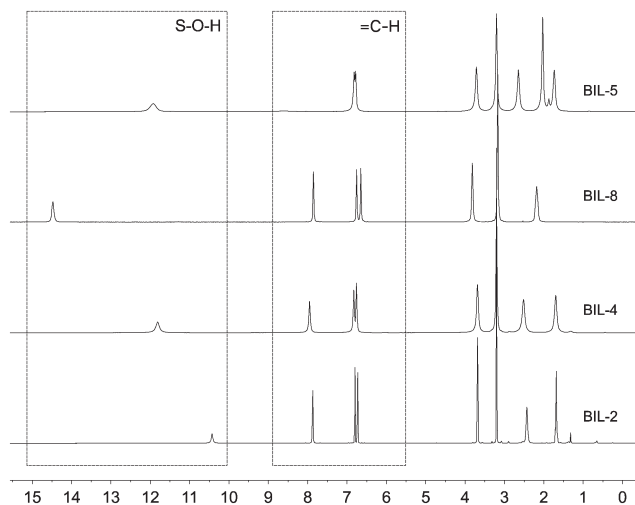


Fig. 4 ^1H NMR spectra (600 MHz, 80 °C, neat) of BIL-2, 4, 5, and 8 (δ : ppm).

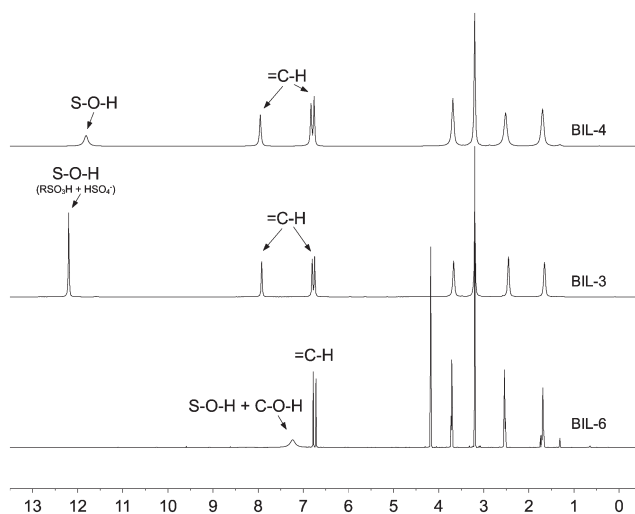


Fig. 5 ^1H NMR spectra (600 MHz, 80 °C, neat) of BIL-3, 4, and 6 (δ : ppm).

This is likely because they are partaking in a strong H-bond, each shared between two oxygen atoms: $\text{S-O-H}\cdots\text{O-S}$ (Fig. 6A). Interestingly, a system of three-centre two protons bonding was probably presented in BIL-6 (Fig. 6B). In these two cases, an intermolecular interaction of an identical H-bond involving two cations cannot be excluded. The significant up-field shifted signal at 7.23 ppm indicates that the protons are prone to interact with the nonbonding electron pair on oxygen of $-\text{CH}_2\text{O}^-$ group. The resistance to exchange between the cluster leads to a broad signal.

Interaction between BILs and nucleophilic TEPO (Gutmann acceptor number). Information on the acceptor number (AN) of BIL could help predict the intermolecular interactions of nucleophiles or electron-rich substrates with the labile protons in BILs. In this study, ANs were determined by $^{31}\text{P}\{^1\text{H}\}$ NMR spectroscopy, using small quantities of the

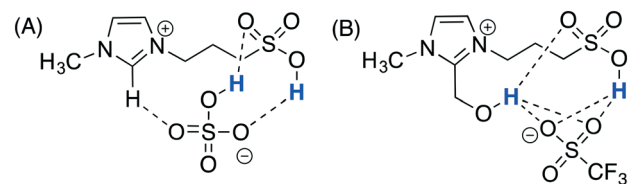


Fig. 6 Schematic diagram of the structural speculation for BIL-3 (A) and BIL-6 (B).

weakly basic probe molecule, TEPO. Changes in the $^{31}\text{P}\{^1\text{H}\}$ NMR chemical shift were induced through the formation of acid–base adducts with partial protonation by Brønsted acids. The recorded $^{31}\text{P}\{^1\text{H}\}$ NMR signals of the protonated probe were found to be slightly concentration-dependent. The ANs, along with the errors derived from the linear extrapolation, are listed and compared in Table 2.

All the BILs studied, except for BIL-7, show high acidity, with ANs falling within the region referred to as super-acidity ($\text{AN} = 114\text{--}118$).²² The ANs measurement of BIL-2 gave two minor $^{31}\text{P}\{^1\text{H}\}$ signals at approximately δ 92 and 85 ppm other than the primary one at δ 81 ppm, indicating that the decomposition of BIL-2 had occurred. This outcome could be rationalized by the sensitivity of its BF_4^- group to nucleophiles, as detected by hydrolysis in the presence of H_2O .²³ The most up-field peak was assigned to the interaction of TEPO with labile protons in BIL-2, generating an AN value of 93.1.

As detected for BIL-2–4, ANs vary significantly by tuning the anion structure, with the value increased with decreasing basicity of the anion ($\text{AN} = 93.1$ (BF_4^-), 115.9 (HSO_4^-), 119.0 (CF_3SO_3^-)). Neither C2–H nor proton in $[\text{HSO}_4^-]$ can compete effectively with $[\text{SO}_3\text{H}]$ for TEPO. However, they may form a strong H-bond towards $[\text{SO}_3\text{H}]$ via $\text{H}\cdots\text{O-S}$, causing an increase in the protonation ability of the labile proton. Consequently, blocking C2–H with a methyl group resulted in a reduced AN for IL-5 (117.5). In contrast, AN of BIL-6 (119.2) was increased slightly by grafting $-\text{CH}_2\text{OH}$ at the C2-position, a stronger H-donor than C2–H. It is also a benefit to introduce a strong electron-withdrawing group to the bridge chain, as evidenced by BIL-8 ($\text{AN} = 119.1$).

Key parameters affect the reaction efficiency. The yield of isosorbide produced using different BIL, and ANs and chemical shift of labile proton in ^1H NMR observed for those BILs are compared in Fig. 7. This demonstrated that the reactivity

Table 2 Water content and Gutmann acceptor number (AN) value of BILs used in this study

BILs	$\chi_{\text{H}_2\text{O}} (\times 10^{-3})$	AN
BIL-2	2	93.1(3)
BIL-3	1	115.9(8)
BIL-4	1	119.0(7)
BIL-5	1	117.5(5)
BIL-6	2	119.2(9)
BIL-8	2	119.1(1)
BIL-9	1	131.7(2)

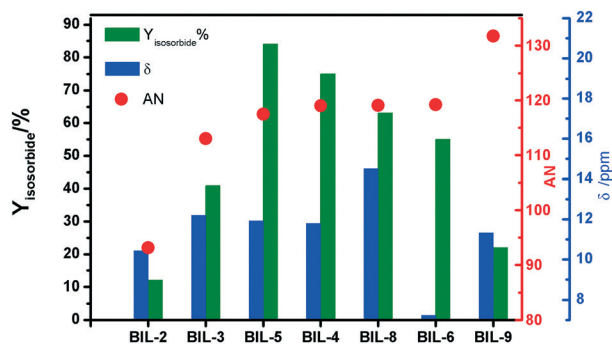


Fig. 7 Yield of isosorbide in reactions catalyzed with AN values and chemical shift (ppm) of proton (600 MHz, 80 °C, neat).

of respective BIL is closely related to its AN value rather than the inherent acidity. Specifically, the yield of isosorbide was first increased, which was followed by a sharp decrease, with increasing AN value. The optimized yield (84.5%) was obtained for BIL-5 with a moderate AN value of 117.5. Remarkably, the mineral acid $\text{CF}_3\text{SO}_3\text{H}$ of a high AN value^{22b} only offered the product in a yield of 16.8%.

Herein, the comparable lower boiling point of $\text{CF}_3\text{SO}_3\text{H}$ (b.p. (1 atm) = 132 °C) and the strict reaction conditions (under 3 kPa at 130 °C) should be considered. Further experiments demonstrated a small amount of acid (ca. 18 ‰ on the basis of the pH value of the removed water) was indeed lost together with the water vapor after reaction for 4 h in the $\text{CF}_3\text{SO}_3\text{H}$ -catalyzed process (Fig. S3†). In comparison, a decreased loss of acid (ca. 12 ‰) was detected for BIL-4 under identical conditions.

The experimental proof of formation of multi-nuclear complex $[\text{SO}_3\text{-H}(\text{H}_2\text{O})_n \cdots \text{anion}]$ for a mixture of H_2O and BIL has been provided by ^1H NMR detection using BIL-4 as an example. The strength of the O–H bond in $[\text{SO}_3\text{H}]$ was weakened significantly, particularly under reaction conditions, rendering proton release in a form of $\text{H}(\text{H}_2\text{O})_n \cdots \text{SO}_3\text{CF}_3$ probable. Evidently, in the presence of stronger nucleophiles, such as DMSO (as the solvent), the labile proton in BIL-4 was removed together with CF_3SO_3^- anion at 50 °C, with the respective zwitterionic precursor generated (Fig. 8).²⁴

Protonation of the formed H_2O and other secondary hydroxyl groups at 1,4-sorbitan occurred coincidentally with that of the desired primary hydroxyl group at the C6 position during the second dehydration. The ability of the acid in proton-

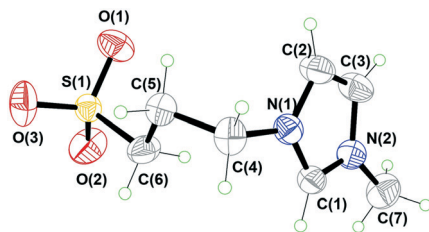


Fig. 8 ORTEP of the zwitterionic precursor of BIL-4 from the X-ray single crystal structure.

ation was increased with a higher AN. However, it was unfavourable to the desired reaction, leading to isosorbide by strengthening either of the two side interactions. In other words, to attain an optimized yield of isosorbide, a proper AN value of the acidic catalyst was required.

Kinetic study on BIL-4-catalyzed dehydration of sorbitol.

Kinetic study on BIL-4-catalyzed dehydration of sorbitol was conducted at 130, 140, and 150 °C (Fig. S4†), respectively, to further understand the structure–performance relationship. The time-course plot at 130 °C was depicted as a typical example in Fig. 9. This demonstrated that only a small amount of isosorbide was formed in the first 1 h regardless of the accumulation of 1,4-sorbitan. Thereafter, the yield of isosorbide increased at an accelerated pace to maximum. This suggests that the reaction is controlled by pre-equilibrium, which is the association equilibrium between the reactant and BIL-4 in this case.

We simulated the time course of sorbitol dehydration by assuming the Michaelis–Menten type mechanism²⁴ involving a pre-equilibrium of association and a subsequent dehydration step based on the important interaction of labile protons in BILs with the substrate (Scheme 1). Herein, k_1 and k_2 are rate constants for the dehydration of sorbitol and 1,4-sorbitan, respectively, whereas k_3 , k_4 , and k_5 are the rate constants for side reactions of sorbitol, 1,4-sorbitan, and isosorbide. In addition, the equilibrium constants for the association of BIL with sorbitol, 1,4-sorbitan, and isosorbide are denoted as K_1 , K_2 , and K_3 , respectively.

The simulation curves fitted well with the experimental data (Fig. 9 and S4†). The proposed kinetic model accurately predicted the product yields with an average deviation of less than 0.2%. The calculated k_3 , k_4 and k_5 were apparently lower than k_1 and k_2 (Table 3), which is in agreement with 1,4-sorbitan and isosorbide being the main products in the reaction. We also found the decomposition rate of isosorbide, which was explained by the constant k_5 , is the lowest, indicating that isosorbide is stable compared to its precursors, such as sorbitol and sorbitans, under the reaction condition. To our surprise, the rate constant k_1 was lower than k_2 at 130 °C.

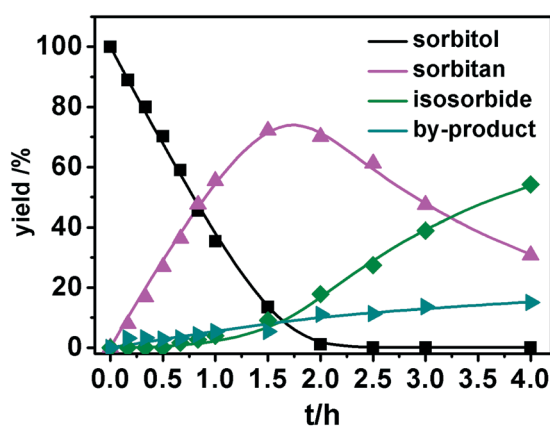
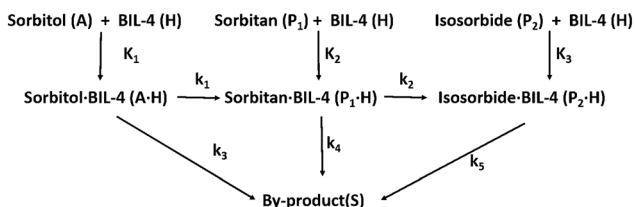


Fig. 9 Experimental (dots) and simulated (lines) profiles for the BIL-4-catalyzed dehydration of sorbitol at 130 °C.



Scheme 1 Reaction schemes of BIL-4-catalyzed dehydration of sorbitol.

Table 3 Rate constants and ratios of the association equilibrium constants

T/°C	130	140	150
k_1/h^{-1}	107.8	240.3	347.7
k_2/h^{-1}	136.6	109.8	98.6
k_3/h^{-1}	9.8	21.1	86.9
k_4/h^{-1}	14.2	12.3	1.8
k_5/h^{-1}	3.9	18.6	27.8
K_1	1.9	1.4	1.3
K_2	0.11	0.27	0.40
K_3	0.1448	0.0009	0.0089

However, the association equilibrium constant of K_1 was greater than that of either K_2 or K_3 , indicating that pre-equilibrium is the key parameter affecting the reaction rate at low temperature, and the association of BIL-4 with sorbitol is stronger than that with 1,4-sorbitan and isosorbide. With increasing reaction temperature, the equilibrium constant K_1 was reduced, concomitantly with a steadily increased K_2 . This outcome suggests that the rate of formation of adducts between sorbitol and 1,4-sorbitan with the acid catalyst is different, which is likely to be crucial to tune the selectivity of dehydration.

Consideration of a continuous process

Recycling study. The recyclability of BIL-4 was examined with each cycle following a sequence of reaction-partial separation by the distillation-fresh input of sorbitol, which mimics a process of the desired continuous reaction. To keep a constant mole ratio of catalyst/sorbitol at 0.6 mol% for each run, the molar quantity of sorbitol of the new feed should be the same as that of isosorbide separated from the previous run. The conversion and selectivity of each group were the average values of at least three samples collected from different areas of the reactor to reduce the experimental error. The results showed that BIL-4 has good catalytic activity in the conversion of sorbitol to isosorbide. In five consecutive runs, both the conversion of sorbitol and yield of isosorbide was relatively stable at about 99% and 73%, respectively (Fig. 10).

Systematic optimization. The pilot-scale process simulations of the dehydration process were carried out using Aspen Plus v7.1. The process contains two key units: continuous stirred tank reactor (CSTR) and evaporator. The conditions were found to be optimal on the basis of dynamic experiments and the documented data of vapor-liquid equilibrium.²⁵ In this study, the treating capacity of sorbitol dehydration plant was assumed to be 5 tons per year.

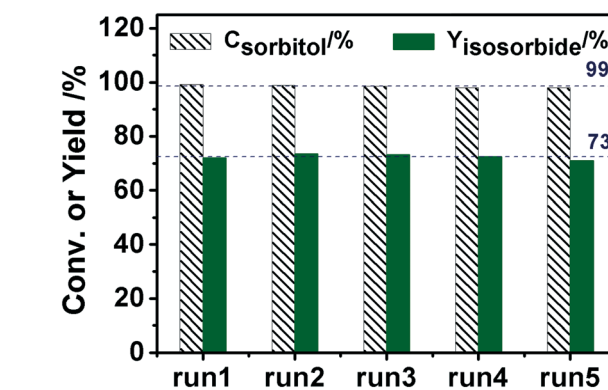


Fig. 10 Conversion of sorbitol and yield of isosorbide from the BIL-4-catalyzed dehydration of sorbitol in consecutive recycling cycles (conditions: BIL-4: 0.6 mol%, 130 °C, 1.5 h).

librium.²⁵ In this study, the treating capacity of sorbitol dehydration plant was assumed to be 5 tons per year.

The process flow diagram for the dehydration process is explained in Fig. 11 and the detail mass balance is shown in Tables S5–S7.† Sorbitol (68 kmol h^{-1}) would be heated to melt as a colorless transparent liquid in the E101 at 120 °C to obtain good flowability. The pretreated sorbitol was then transferred into the R101 where isosorbide and 1,4-sorbitan could be produced in the presence of BIL-4 at the optimized temperature of 160 °C and under a pressure of 4 kPa. As calculated, the optimal retention time of the reaction mixture in R101 was 90 min. Thereafter, it was transferred to V101 for proceeding distillation at 230 °C under 4 kPa for 10 min to obtain the raw isosorbide as a lighter composition. Notably, a type of reaction-distillation was considered during this simulation. 80 wt% of the heavier composition in V101 including both by-product and catalyst was backflow into R101 for further reaction with the fresh input of substrate (68 kmol h^{-1}) and catalyst (8.16 mol h^{-1}). This demonstrated that a yield of 82% of isosorbide with a purity of 99.3% could be reached at balance by this continuous process; this result and process is

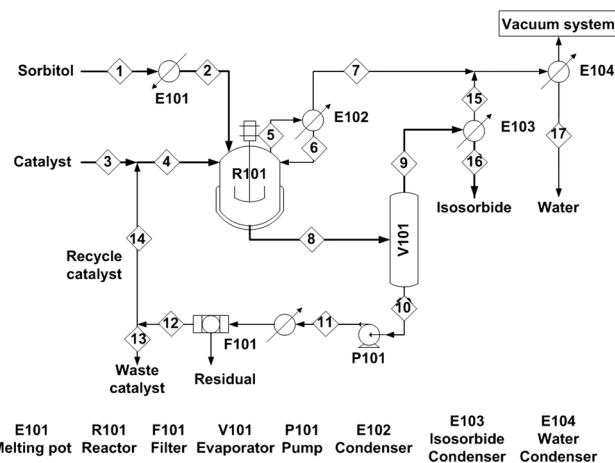


Fig. 11 Process flow diagram of the dehydration process.

much higher and more efficient than that obtained by the traditional batch process.²⁶

Conclusions

In summary, the structure–performance of BIL-catalyzed dehydrative formation of isosorbide from sorbitol was explored extensively, thereby offering an efficient, eco-friendly and reusable catalyst. Kinetic studies demonstrated that such sequential steps are different in the rate of formation of adducts between sorbitol and 1,4-sorbitan with the acid. The remarkable difference in performance in the second dehydration of various BILs was attributed to their respective ability to protonate polyhydroxyl substrates. Consequently, a proper value of AN rather than the inherent of acidity was found to be essential for an optimized yield of isosorbide. A continuous process was finally constructed upon system optimization using the preferred BIL-4 as the catalyst, which generated a yield of 82% in isosorbide with a purity of 99.3% at balance.

Acknowledgements

Financial support by the National Basic Research Program of China (973 Program) 2015CB251401, the National Natural Science Foundation of China (No. 21476240, 21606238, 21374029), the Instrument Developing Project of the Chinese Academy of Sciences (No. YZ201521), the Shanghai education commission key projects of scientific research and innovation (14ZZ061), the Key Research Program of Frontier Sciences, CAS (QYZDY-SSW-JSC011), CAS (Chinese Academy of Sciences) 100-Talent Program (2014), and Key Research Program of Frontier Sciences, CAS (QYZDY-SSW-JSCo11) is gratefully acknowledged.

Notes and references

- (a) S. P. Collins, P. D. Levy and J. L. Martindale, *et al.*, *Acad. Emerg. Med.*, 2016, **23**, 922–931; (b) I. S. Anand, S. W. Tam and W. T. Archambault, *Circulation*, 2005, **112**, 704.
- (a) Y. Zhu, M. Durand and V. Molinier, *et al.*, *Green Chem.*, 2008, **10**, 532–540; (b) B. S. Rajput, S. R. Gaikwad and S. K. Menon, *et al.*, *Green Chem.*, 2014, **16**, 3810–3818; (c) C. C. Chien and J. H. Liu, *Langmuir*, 2015, **31**, 13410–13419; (d) P. Barbaro, F. Liguori and C. Moreno-Marrodan, *Green Chem.*, 2016, **18**, 2935–2940.
- (a) F. Fenouillot, A. Rousseau and G. Colomines, *et al.*, *Prog. Polym. Sci.*, 2010, **35**, 578–622; (b) P. A. Fokou and M. A. R. Meier, *J. Am. Chem. Soc.*, 2009, **131**, 1664–1665; (c) R. M. Gohil, *Polym. Eng. Sci.*, 2009, 543–553.
- R. Steinmetz and N. A. Mitchner, *et al.*, *Endocrinology*, 1998, **139**, 2741–2747.
- (a) Y. Li, Y. Liao and X. Cao, *et al.*, *Biomass Bioenergy*, 2015, **74**, 148–161; (b) F. Aricò and P. Tundo, *J. Org. Chem.*, 2016, **12**, 2256–2266; (c) M. E. Zakrzewska, E. Bogel-Lukasik, R. Bogel-Lukasik and R. Bogel-Lukasik, *Chem. Rev.*, 2011, **111**, 397–417.
- (a) L. Došen-Mićović and Ž. Čeković, *J. Phys. Org. Chem.*, 1998, **11**, 887–894; (b) Ž. Čeković and J. Serb, *J. Serb. Chem. Soc.*, 1986, **51**, 205–211; (c) R. Barker, *J. Org. Chem.*, 1970, **35**, 461–464.
- (a) K. Bock, C. Pedersen and H. Thogersen, *Acta Chem. Scand., Ser. B*, 1981, **35**, 441–449; (b) R. C. Hockett, H. G. Fletcher Jr. and E. L. Sheffield, *et al.*, *J. Am. Chem. Soc.*, 1946, **68**, 927–930.
- (a) G. Fleche and M. Huchette, *Starch/Staerke*, 1986, **38**, 26–30; (b) J. M. Robinson, A. M. Wadle and M. D. Reno, *et al.*, *Energy Fuels*, 2015, **29**, 6529–6535; (c) D. J. Schreck, M. M. K. Bradford and N. A. Clinton, *et al.*, *US pat.* US20090259057, 2009; (d) A. A. Dabbawala, D. K. Mishra and G. W. Huber, *et al.*, *Appl. Catal., A*, 2015, **492**, 252–261; (e) J. Li, A. Spina and J. A. Moulijn, *et al.*, *Catal. Sci. Technol.*, 2013, **3**, 1540–1546; (f) A. Yamaguchi, N. Hiyoshi and O. Sato, *et al.*, *Green Chem.*, 2011, **13**, 873–881.
- (a) B. Op de Beeck, J. Geboers and S. Van de Vyver, *et al.*, *ChemSusChem*, 2013, **6**, 399; (b) J. Xi, Y. Zhang and D. Ding, *et al.*, *Appl. Catal., A*, 2014, **469**, 108–115; (c) A. A. Dabbawala, D. K. Mishra and J. S. Hwang, *Catal. Commun.*, 2013, **42**, 1–5; (d) A. Yamaguchi, N. Hiyoshi and O. Sato, *et al.*, *Green Chem.*, 2011, **13**, 873–881.
- J. Xia, D. Yu and Y. Hu, *et al.*, *Catal. Commun.*, 2011, **12**, 544–547.
- M. Kurszewska, E. Skorupowa and J. Madaj, *et al.*, *Carbohydr. Res.*, 2002, **337**, 1261–1268.
- P. Sun, D. H. Yu and H. Huang, *et al.*, *Korean J. Chem. Eng.*, 2011, **28**, 99–105.
- X. Zhang, D. Yu, J. Zhao and H. Huang, *et al.*, *Catal. Commun.*, 2014, **43**, 29–33.
- J. Xi, Y. Zhang and D. Ding, *et al.*, *Appl. Catal., A*, 2014, **469**, 108–115.
- M. Gu, D. Yu and H. Zhang, *et al.*, *Catal. Lett.*, 2009, **133**, 214–220.
- (a) A. K. Chakraborti and S. R. Roy, *J. Am. Chem. Soc.*, 2009, **131**, 6902; (b) Q. Wang and X. Yao, *et al.*, *Green Chem.*, 2012, **14**, 2559–2566; (c) K. Matuszek, A. Chrobok and F. Coleman, *et al.*, *Green Chem.*, 2014, **16**, 3463–3471; (d) J. Banothu, R. Gali and R. Velpula, *et al.*, *J. Chem. Sci.*, 2013, **125**, 843–849; (e) S. J. Zhang, J. Sun and X. Zhang, *et al.*, *Chem. Soc. Rev.*, 2014, **43**, 7838–7869.
- (a) A. K. Chakraborti and S. R. Roy, *J. Am. Chem. Soc.*, 2009, **131**, 6902; (b) Q. Wang, X. Yao and S. Tang, *et al.*, *Green Chem.*, 2012, **14**, 2559–2566; (c) K. Matuszek, A. Chrobok and F. Coleman, *et al.*, *Green Chem.*, 2014, **16**, 3463–3471; (d) A. M. da Costa Lopes and R. Bogel-Lukasik, *ChemSusChem*, 2015, **8**, 947–965; (e) A. M. da Costa Lopes and R. Bogel-Lukasik, *Green Chem.*, 2014, **16**, 1617–1627; (f) S. Zhang, J. Sun and X. Zhang, *et al.*, *Chem. Soc. Rev.*, 2014, **43**, 7838–7869.
- (a) C. Lansalot-Matras and C. Moreau, *Catal. Commun.*, 2003, **4**, 517–520; (b) Y. N. Li, J. Q. Wang and L. N. He, *et al.*, *Green Chem.*, 2012, **14**, 2752–2758; (c) H. Li, W. J. Xu and T. Huang, *et al.*, *ACS Catal.*, 2014, **4**, 4446–4454; (d) C. Shi, Y.

- Zhao and J. Xin, *et al.*, *Chem. Commun.*, 2012, **48**, 4103–4105; (e) S. Peleteiro, C. Shi, Y. Zhao and J. Xin, *et al.*, *Ind. Eng. Chem. Res.*, 2015, **54**, 8368–8373; (f) A. V. Carvalho, A. M. da Costa Lopes and R. Bogel-Lukasik, *RSC Adv.*, 2015, **5**, 47153–47164.
- 19 (a) M. J. Earle, J. M. S. S. Esperanca and M. A. Gilea, *et al.*, *Nature*, 2006, **439**, 831–834; (b) J. Sun, X. Yao and W. Cheng, *et al.*, *Green Chem.*, 2014, **16**, 3297–3304; (c) S. Chen, S. Zhang and X. Liu, *et al.*, *Phys. Chem. Chem. Phys.*, 2014, **16**, 5893–5906; (d) K. Dong, S. Zhang and J. Wang, *Chem. Commun.*, 2016, **62**, 6744–6764.
- 20 M. Yabushita, H. Kobayashi, A. Shrotri, K. Hara, S. Ito and A. Fukuoka, *Bull. Chem. Soc. Jpn.*, 2015, **88**, 996–1002.
- 21 M. A. Zolfigol, A. Khazaei and A. R. Moosavi-Zare, *et al.*, *J. Org. Chem.*, 2012, **77**, 3640–3645.
- 22 (a) M. Schmeisser, P. Illner and R. Puchta, *et al.*, *Chem. – Eur. J.*, 2012, **18**, 10969–10982; (b) J. A. McCune, P. He and M. Petkovic, *et al.*, *Phys. Chem. Chem. Phys.*, 2014, **16**, 23233–23243; (c) M. Holzweber, R. Lungwitz and D. Doerfler, *et al.*, *Chem. – Eur. J.*, 2013, **19**, 288–293; (d) R. Lungwitz, M. Friedrich and W. Linert, *et al.*, *New J. Chem.*, 2008, **32**, 1493–1499.
- 23 (a) R. P. Swatloski, J. D. Holbrey and R. D. Rogers, *Green Chem.*, 2003, **5**, 361–363; (b) M. G. Freire, C. M. S. S. Neves and I. M. Marrucho, *et al.*, *J. Phys. Chem. A*, 2010, **114**, 3744–3749; (c) J. G. Huddleston, A. E. Visser and W. M. Reichert, *et al.*, *Green Chem.*, 2001, **3**, 156–164; (d) P. Wasserscheid, R. van Hal and A. Bösmann, *Green Chem.*, 2002, **4**, 400–404.
- 24 X. M. Liu, Z. X. Song and H. J. Wang, *Struct. Chem.*, 2009, **20**, 509.
- 25 Y. S. Xie, *Preparation and Purification Process study on Isosorbide*, Nanjing: Nanjing University of Technology, 2010, 7 (thesis: <http://www.docin.com/p-896109494.html>).
- 26 K. M. Moore and A. J. Sanborn, *US pat.*, US6849748 B2, 2005; L. A. Hartmann, *US Pat.*, 3454603, 1969.